REGULAR ARTICLE

blood advances

Ablation of collagen VI leads to the release of platelets with altered function

Vittorio Abbonante,[1,2] Cristian Gruppi,[1,2] Monica Battiston,[3,*] Alessandra Zulian,[4,*] Christian Andrea Di Buduo,[1,2,*] Martina Chrisam,[5] Lucia Sereni,[6] Pierre-Alexandre Laurent,[1,2] Claudio Semplicini,[7] Elisabetta Lombardi,[3] Mario Mazzucato,[3] Francesco Moccia,[8] Valeria Petronilli,[4] Anna Villa,[6,9] Luca Bello,[7] Elena Pegoraro,[7] Paolo Bernardi,[4] Paola Braghetta,[5] Luigi De Marco,[3,10] Paolo Bonaldo,[5] and Alessandra Balduini[1,2,11]

[1]Department of Molecular Medicine, University of Pavia, Pavia, Italy; [2]Laboratory of Biochemistry-Biotechnology and Advanced Diagnostics, Istituto di Ricovero e Cura a Carattere Scientifico Policlinico San Matteo Foundation, Pavia, Italy; [3]Stem Cell Unit, Centro di Riferimento Oncologico di Aviano, Istituto di Ricovero e Cura a Carattere Scientifico, Aviano, Italy; [4]Department of Biomedical Sciences and Consiglio Nazionale delle Ricerche, Neuroscience Institute, University of Padova, Padova, Italy; [5]Department of Molecular Medicine, University of Padova, Padova, Italy; [6]Telethon Institute for Gene Therapy, Division of Regenerative Medicine, Stem Cells, and Gene Therapy, Istituto di Ricovero e Cura a Carattere Scientifico, San Raffaele Scientific Institute, Milan, Italy; [7]Department of Neurosciences, University of Padova, Padova, Italy; [8]Department of Biology and Biotechnology, University of Pavia, Pavia, Italy; [9]Milan Unit, Istituto di Ricerca Genetica e Biomedica, Consiglio Nazionale delle Ricerche, Milan, Italy; [10]Department of Molecular and Experimental Medicine, Scripps Research Institute, La Jolla, CA; and [11]Department of Biomedical Engineering, Tufts University, Medford, MA

Key Points

- Megakaryocytes express collagen VI that regulates the release of functional platelets.
- Collagen VI–null megakaryocytes and platelets display increased mTOR signaling and store-operated calcium entry.

Hemostatic abnormalities and impaired platelet function have been described in patients affected by connective tissue disorders. We observed a moderate bleeding tendency in patients affected by collagen VI–related disorders and investigated the defects in platelet functionality, whose mechanisms are unknown. We demonstrated that megakaryocytes express collagen VI that is involved in the regulation of functional platelet production. By exploiting a collagen VI–null mouse model (*Col6a1*$^{-/-}$), we found that collagen VI–null platelets display significantly increased susceptibility to activation and intracellular calcium signaling. *Col6a1*$^{-/-}$ megakaryocytes and platelets showed increased expression of stromal interaction molecule 1 (STIM1) and ORAI1, the components of store-operated calcium entry (SOCE), and activation of the mammalian target of rapamycin (mTOR) signaling pathway. In vivo mTOR inhibition by rapamycin reduced STIM1 and ORAI1 expression and calcium flows, resulting in a normalization of platelet susceptibility to activation. These defects were cell autonomous, because transplantation of lineage-negative bone marrow cells from *Col6a1*$^{-/-}$ mice into lethally irradiated wild-type animals showed the same alteration in SOCE and platelet activation seen in *Col6a1*$^{-/-}$ mice. Peripheral blood platelets of patients affected by collagen VI–related diseases, Bethlem myopathy and Ullrich congenital muscular dystrophy, displayed increased expression of STIM1 and ORAI1 and were more prone to activation. Altogether, these data demonstrate the importance of collagen VI in the production of functional platelets by megakaryocytes in mouse models and in collagen VI–related diseases.

Introduction

Collagen VI is an extracellular matrix protein that forms a distinct microfibrillar network and plays a remarkably broad range of key roles in different tissues. These include cytoprotection by counteracting apoptosis and oxidative damage, regulation of autophagy and cell differentiation, contribution to stem cell

Submitted 26 January 2021; accepted 12 July 2021; prepublished online on *Blood Advances* First Edition 21 September 2021; final version published online 6 December 2021. DOI 10.1182/bloodadvances.2020002671.

*M.B., A.Z., and C.A.D.B. contributed equally to this study.

Data sharing requests should be sent to Alessandra Balduini (alessandra.balduini@unipv.it).

The full-text version of this article contains a data supplement.

self-renewal and tissue regeneration, and promotion of tumor growth and progression.[1] In humans, the major form of collagen VI is made up of 3 genetically distinct chains, α1(VI), α2(VI), and α3(VI), that are coded by the *COL6A1*, *COL6A2*, and *COL6A3* genes, respectively.[1] More recently, 3 additional genes (*COL6A4*, *COL6A5*, and *COL6A6*) were identified that code for other collagen VI chains that can substitute for α3(VI).[2,3] Mutations in collagen VI genes in humans have been linked to a broad spectrum of muscular and neurological diseases, including Bethlem myopathy, Ullrich congenital muscular dystrophy (UCMD), congenital myosclerosis, and early-onset isolated dystonia.[1,4] Different from other muscular dystrophies, collagen VI–related myopathies display remarkable alterations of the extracellular matrix of muscle and other connective tissues, including joints, tendons, and skin, and they can be considered hybrid disorders with clinical manifestations attributable to muscle and connective tissues.[4]

The crucial roles exerted by collagen VI in vivo have been unveiled mainly by exploiting the collagen VI–null (*Col6a1*$^{-/-}$) mouse model, which was generated by targeted inactivation of the *Col6a1* gene, resulting in the prevention of assembly and secretion of the entire collagen VI protein.[5] Different studies, aimed at dissecting the pathomolecular defects underlying the myopathic phenotype of *Col6a1*$^{-/-}$ mice, revealed several alterations in the mitochondria and the sarcoplasmic reticulum, 2 organelles that are primarily involved in maintaining intracellular calcium (Ca^{2+}) homeostasis.[6,7] The pathomolecular alterations characterizing the muscles of *Col6a1*$^{-/-}$ mice have recently been found in other cells and tissues.[1,8-10]

Some studies and case reports have described hemostatic abnormalities and platelet function defects in patients affected by heritable connective tissue disorders, such as collagenopathies.[11-13] When assessing the blood parameters of patients affected by Bethlem myopathy and UCMD, we observed a mild bleeding tendency, suggesting a defect in platelet functionality. These findings led us to broaden the exploration of the defects caused by collagen VI mutations in the circulatory system.

Intracellular Ca^{2+} signaling is a fundamental regulator of megakaryocyte (Mk) and platelet function through modulation of several intracellular pathways.[14-18] Store-operated calcium entry (SOCE) is a well-described mechanism regulating Ca^{2+} entry from the extracellular space following endoplasmic reticulum (ER) store depletion.[19] We and other investigators have previously described the expression and function of SOCE in Mks and platelets.[16,20-22] Mks express the 2 molecular components of SOCE, the ER Ca^{2+} sensor stromal interaction molecule 1 (STIM1) and the plasma membrane Ca^{2+} channel ORAI1, which are activated upon depletion of the intracellular Ca^{2+} pool. Ca^{2+} mobilization from the intracellular stores promotes Mk function and proplatelet extension.[16] In platelets, STIM1 and ORAI1 have been demonstrated to drive activation processes in response to agonists.[15,23-25] The phosphatidylinositol 3-kinase (PI3K)/Akt/mammalian target of rapamycin (mTOR) axis is an intracellular signaling pathway enhanced by SOCE.[26] In turn, mTOR regulates the expression of SOCE components.[27,28] The PI3K/Akt/mTOR axis plays a pivotal role in regulating Mk and platelet function by controlling Mk proliferation and differentiation and platelet activation and aggregation, respectively.[29-32] In addition to its role in Mk and platelet function, the PI3K/Akt/mTOR axis is known to be a crucial regulator of collagen I expression.[33,34]

Here, we exploited the collagen VI–null mouse model by generating Mk culture and radiation chimeras using bone marrow (BM) lineage-negative (Lin^-) cell transplantations. We also investigated platelet function in *Col6a1*$^{-/-}$ mice and in samples from patients affected by collagen VI–related disorders.

Methods

Commercial antibodies used are listed in supplemental Table 1. Primers for human and mouse collagen VI are listed in supplemental Table 2.

Information about reagents, platelet preparation, platelet aggregation, reverse transcription polymerase chain reaction (RT-PCR), western blotting, intracellular Ca^{2+} measurements in platelets, tissue collection and immunofluorescence, and BM transplant are provided in supplemental materials.

Cell cultures

Human Mks were obtained by differentiating cord blood–derived $CD34^+$ or peripheral blood–derived $CD45^+$ hematopoietic progenitors, as described previously.[35,36] Mouse Mks were obtained by differentiating BM cells for 4 days in Dulbecco's modified Eagle medium (Gibco) supplemented with 1% penicillin/streptomycin, 1% L-glutamine, and 10% fetal bovine serum (Gibco), in the presence of 10 ng/mL recombinant murine thrombopoietin (PeproTech). On day 4, mature Mks were isolated by bovine serum albumin gradient sedimentation. For in vitro treatment with the prolyl-4 hydroxylase inhibitor ethyl 3,4-dihydroxybenzoate (EDHB), Mks were cultured for 24 hours with 100 μM EDHB or with vehicle alone (0.1% ethanol). For in vitro treatment with ascorbic acid, Mks were cultured in the presence of 50 μg/mL ascorbic acid for 48 hours. For in vitro treatment with rapamycin, BM cells were cultured at day 0 for 4 days in the presence of 100 nM rapamycin or 0.1% dimethyl sulfoxide (DMSO) as vehicle control.

Flow cytometry

Stim1 and ORAI1 staining. To analyze STIM1 and ORAI1 in BM Mks, femurs were flushed, and red blood cells were lysed with 0.8% ammonium chloride solution. The remaining cells were washed by centrifugation with phosphate-buffered saline and stained with anti-ORAI1 antibody (1:100; Santa Cruz Biotechnologies) or anti-STIM1 antibody (1:100; Abcam). For STIM1 staining, cells were permeabilized with commercial buffers (BD Pharmingen) prior to staining with the antibody. To recognize BM Mks, we costained cells with an anti-CD41 antibody (0.1 mg/mL; BioLegend). All Mk samples were characterized as CD41/CD42b-positive and CD3/CD4/CD8/CD11b/CD19/CD33-negative cells, using appropriate antibodies (0.1 mg/mL; all from Beckman Coulter). Samples were acquired with a FACSDiva flow cytometer (Beckman Coulter). The analytical gating was set using unstained samples and relative isotype controls. Offline data were analyzed using the Beckman Coulter Kaluza software package (Beckman Coulter) and Flowing software 2.5.1 (University of Turku).

BM Mk sorting. Mks were sorted from BM cells as the $CD11b^-$/$CD61^+$/$CD9^+$ population.[37] The gating strategy is shown in supplemental Figure 9. Mk purity after sorting, by means of $CD61^+$/$CD9^+$/$CD41^+$, was routinely performed and assessed to be >95%. Cell viability was checked using Trypan Blue solution (Sigma Aldrich). Cell sorting experiments were performed using a

FACSAria IIu (3 lasers; BD Bioscience). FACSDiva software (BD Pharmingen) was used for data acquisition and analysis.

Platelet activation. For platelet activation, 2×10^6 platelets washed in modified Tyrode's buffer (134 mM NaCl, 0.34 mM Na_2HPO_4, 2.9 mM KCl, 12 mM $NaHCO_3$, 20 mM HEPES, 5 mM glucose) containing 1 mM $CaCl_2$ were incubated with 0.1 U/mL thrombin (Sigma-Aldrich), 25 μM adenosine diphosphate (ADP; Sigma-Aldrich), 20 ng/mL convulxin (Enzo Life Sciences), or vehicle alone in the presence of 2 μg/mL JON/A-PE (Emfret Analytics), 12 μg/mL PAC-1–FITC (BD Biosciences), or 10 μg/mL anti-CD62P–APC (BioLegend) and analyzed 10 minutes later.[38] Platelet activation was expressed as the ratio between the mean fluorescence intensity measured after the stimulation with each agonist and the mean fluorescence intensity measured after incubation with vehicle alone.[39]

Intracellular Ca^{2+} measurements in Mks

To study SOCE, Mks were treated with 10 mM cyclopiazonic acid (CPA) in Ca^{2+}-free (Ca^{2+} 0) solution to deplete the stores. Similar to thapsigargin treatment, CPA treatment causes a transient increase in the intracellular Ca^{2+} concentration $[Ca^{2+}]_i$ due to the passive emptying of Ca^{2+} stores. After Ca^{2+} levels return to baseline, external Ca^{2+} is restored to 1.5 mM, causing a second increase in intracellular Ca^{2+} levels due to activated SOCE. As an internal control, Mks were treated with vehicle alone (0.03% volume-to-volume ratio of DMSO), which did not elicit any significant increase in $[Ca^{2+}]_i$ (supplemental Figure 10). Intracellular Ca^{2+} measurements in Mks were performed as previously described.[16,40] For a detailed description, please refer to supplemental Methods.

Mice and in vivo treatments

We performed experiments in wild-type (WT) mice of the inbred C57BL/6NCrl strain and in *Col6a1*$^{-/-}$ mice that we previously backcrossed on the C57BL/6NCrl strain for 8 generations, as previously described.[7] We obtained data for 3-month-old mice by comparing sex-matched WT and *Col6a1*$^{-/-}$ animals. Mouse procedures were approved by the Italian Ministry of Health (approvals #282-2017 and #877-2018). For in vivo treatment with rapamycin, mice were injected intraperitoneally with rapamycin (2 mg/kg body weight) every 24 hours for 14 days, as previously described.[41] Control mice were injected intraperitoneally with vehicle alone (5% PEG-400/5% Tween-80 in saline).

Patient samples

All relevant data concerning symptoms at disease onset, clinical features at last clinical evaluation, disease progression, and genetic analysis are reported in Table 1.

Two males (M) and 3 females (F) belonging to 3 families were studied. Four patients were affected by Bethlem myopathy and 1 had UCMD intermediate [the phenotype was defined upon loss of ambulation by 20 years and start of noninvasive ventilation by 20 years (patient 2/M)].[42] Laboratory tests revealed a normal platelet count in all patients (Table 1). Hemoglobin, hematocrit, and white blood cells were also normal. A structured interview was conducted with all patients using the International Society on Thrombosis and Hemostasis - Bleeding Assessment Tool (Table 1)[43]. Three members of the same kindred (patients 1/F, 4/F, and 5/F) presented with menorrhagia and mild trauma-related bruises, 2 patients (4/F and 5/F) presented with mild oral cavity bleeding, and 1 patient (4/F) also presented with postpartum hemorrhage. According to the cutoff values set by the International Society on Thrombosis and Hemostasis (≥4 in adult males, ≥6 in adult females),[44] only patient 5/F showed an increased risk for bleeding. No arterial or venous thrombosis was observed in our cohort of patients.

Study approval

Human cord blood samples were processed following guidelines of the Ethics Committee of the Istituto di Ricovero e Cura a Carattere Scientifico (IRCCS), Policlinico San Matteo foundation of Pavia and the principles of the Declaration of Helsinki. Five subjects were selected from a cohort of patients with Bethlem myopathy or UCMD who were followed at the Neuromuscular Center of the University of Padova. The study was conducted in accordance with the ethics rules and guidelines issued by the local Ethics Committee and the Declaration of Helsinki. Every patient provided written informed consent. Mouse procedures were approved by the Italian Ministry of Health (approvals #282-2017 and #877-2018).

Statistics

Data are expressed as mean ± standard deviation (SD) or standard error of the mean (SEM). A 2-tailed Student *t* test was used for comparisons between 2 groups. For comparisons of 1 factor across multiple groups, 1-way ANOVA was performed followed by the post hoc Tukey test. GraphPad Prism 8 (GraphPad Software) was used for statistical analyses and graphing. *P* values $< .05$ were considered statistically significant. All experiments were independently replicated ≥3 times.

Results

Human and mouse Mks express collagen VI

To investigate collagen VI expression, human Mks were differentiated from cord blood, whereas mouse Mks were derived from BM progenitors. As shown in Figure 1, Mks of human and murine origin expressed the 3 major collagen VI chains (α1, α2, α3) at RNA (Figure 1A) and protein (Figure 1B) levels. To confirm the specificity of the protein bands, Mks were treated for 24 hours with the prolyl-4 hydroxylase inhibitor EDHB.[45] This treatment reduced the synthesis of collagen VI chains in human and murine Mk cultures with respect to treatment with vehicle alone (Figure 1B). Mature murine Mks cultured in the presence of ascorbic acid were able to secrete collagen VI, which localized around the cell membrane and was also detectable in the culture medium by immunoblotting (Figure 1C-D).

Platelets from collagen VI–null mice are more susceptible to activation

We studied the ex vivo functionality of platelets from WT and *Col6a1*$^{-/-}$ mice. The absence of the collagen VI α1 chain in *Col6a1*$^{-/-}$ Mks was confirmed by western blot analysis (supplemental Figure 1). Collagen VI–null platelets showed an increased tendency toward activation and aggregation. Platelets from *Col6a1*$^{-/-}$ mice exhibited increased levels of activated integrin αIIbβ3 and CD62P (P-selectin) exposure on the cell membrane after stimulation with thrombin, ADP, or the GPVI collagen receptor agonist convulxin (CVX) (Figure 2A). On the other hand, the expression levels of integrin αIIbβ3, PAR-4, P2Y12, and GPVI were not different between WT and *Col6a1*$^{-/-}$ platelets (supplemental

Table 1. Summary of the clinical features, genetic characterization, and International Society on Thrombosis and Hemostasis-Bleeding Assessment Tool for patients with Bethlem myopathy or UCMD included in this study

	Patient 1/F	Patient 2/M	Patient 3/M	Patient 4/F	Patient 5/F
Clinical phenotype	BetMy AD	UCMD intermediate	BetMy	BetMy AD	BetMy AD
Onset					
Age	Adolescence	Neonatal	Neonatal	Adolescence	Childhood
Symptoms	Difficulties in sport	Hypotonia, respiratory distress	Hypotonia, finger contractures	Shoulder and knee dislocation	Slower than peers
Last evaluation					
Age	20	20	18	47	54
Best motor function	Run	WCB (8 y)	Run	Walk	Walk
COL6A mutations	COL6A3: c.5035G>T; p.Gly1679Trp	COL6A1: c.930 + 189C>T, intron 11	COL6A3: c.4859C>T, p.Pro1620Leu (pseudohomozygosity)	COL6A3: c.5035G>T; p.Gly1679Trp	COL6A3: c.5035G>T; p.Gly1679Trp
Platelet count ($\times 10^9$/L)*	251	269	212	267	237
Bleeding phenotype	Menorrhagia, mild trauma-related bruises	Not applicable	Not applicable	Menorrhagia, mild trauma-related bruises, mild oral cavity bleeding, postpartum hemorrhage	Menorrhagia, mild trauma-related bruises, mild oral cavity bleeding
ISTH-BAT[43]	2	0	0	4	7

AD, autosomal dominant; BetMy, Bethlem myopathy; ISTH-BAT, International Society on Thrombosis and Hemostasis-Bleeding Assessment Tool; WCB, wheelchair bound.
*Normal value: 200 to 450 $\times 10^9$/L.

Figure 2). *Col6a1*$^{-/-}$ platelets displayed more avidity for adhesion to collagen I and fibrinogen than did WT platelets (supplemental Figure 3). In vitro *Col6a1*$^{-/-}$ platelet stimulation with the platelet agonists collagen, thrombin, or ADP plus adrenaline led to a robust amplification of the aggregation, thus confirming their hyperreactive behavior (Figure 2B).

Collagen VI–null platelets and Mks have increased levels of SOCE effectors

Platelet activation is directly dependent on the increase in $[Ca^{2+}]_i$ due to SOCE activation.[21] To assess whether the alterations observed in *Col6a1*$^{-/-}$ platelets may depend on changes in the molecular components of SOCE, we analyzed the expression of STIM1, the ER Ca^{2+} sensor, and ORAI1, a plasma membrane Ca^{2+} channel, which detect any significant decrease in ER Ca^{2+} levels and mediate the ensuing extracellular Ca^{2+} entry, respectively.[19] The protein levels of both SOCE effectors were significantly increased in circulating platelets from *Col6a1*$^{-/-}$ mice compared with WT mice (Figure 3A). We exposed cells to thapsigargin to evaluate the impact of increased STIM1 and ORAI1 expression on SOCE function.[46] Thapsigargin blocks the activity of Sarco/Endoplasmic Reticulum Ca^{2+} ATPase (SERCA), thereby preventing Ca^{2+} sequestration into the stores and leading to their depletion, with consequent SOCE activation.[47] In Ca^{2+}0 conditions, the Ca^{2+} mobilization from intracellular stores induced by thapsigargin treatment was similar between WT and *Col6a1*$^{-/-}$ platelets. The addition of extracellular Ca^{2+} in the presence of thapsigargin resulted in a massive Ca^{2+} entry from the extracellular space, which was significantly higher in *Col6a1*$^{-/-}$ platelets (Figure 3B). To evaluate whether these alterations were inherited from Mks or acquired by platelets, we sorted BM Mks and analyzed the expression of STIM1 and ORAI1 transcripts. We found that the levels of both messenger RNAs (mRNAs) were significantly increased in BM Mks from *Col6a1*$^{-/-}$ mice compared with WT mice (Figure 3Ci). These data were further supported by the analysis of STIM1 and ORAI1 protein levels in BM Mks by flow cytometry (Figure 3Cii). The increase in STIM1 and ORAI1 expression in *Col6a1*$^{-/-}$ Mks resulted in an elevation in SOCE-dependent Ca^{2+} signaling. In the absence of extracellular Ca^{2+}, treatment of Mks with CPA, an inhibitor of SERCA that is structurally unrelated to thapsigargin, induced mobilization of Ca^{2+} from the intracellular stores that was comparable between WT and *Col6a1*$^{-/-}$ Mks. Conversely, the addition of extracellular Ca^{2+} in the presence of CPA elicited a significant increase in Ca^{2+} entry from the extracellular space in *Col6a1*$^{-/-}$ Mks (Figure 3D), thus confirming the increase in SOCE.

Altered mTORC1 signaling in collagen VI–null Mks and platelets

It was demonstrated previously that the mTOR signaling axis regulates Mk growth and platelet activation,[29-31] as well as STIM1 and ORAI1 expression.[27,28] Based on this information, we investigated the activation of Akt and the downstream effectors of the mTORC1 signaling complex, S6 and 4E-BP1, in mouse BM Mks and circulating platelets. All of these proteins were significantly more phosphorylated in BM Mks (Figure 4A; supplemental Figure 4) and resting platelets (Figure 4B) derived from *Col6a1*$^{-/-}$ mice compared with WT mice.

Collagen VI–null Mks and platelets maintain SOCE alterations after BM transplantation in WT recipient mice

We investigated whether the alterations in SOCE expression and function in *Col6a1*$^{-/-}$ Mks and platelets were due to the lack of collagen VI in the BM environment or to the intrinsic absence of self-produced collagen VI in Mks. Lin^- BM cells isolated from WT and *Col6a1*$^{-/-}$ donor mice were transplanted into lethally irradiated WT recipient mice. All mice except 1 survived the transplant and recovered their body weight with no signs of clinical suffering. All analyzed mice restored their white blood cell count, indicating a full engraftment of transplanted cells. Mks were then sorted from BM

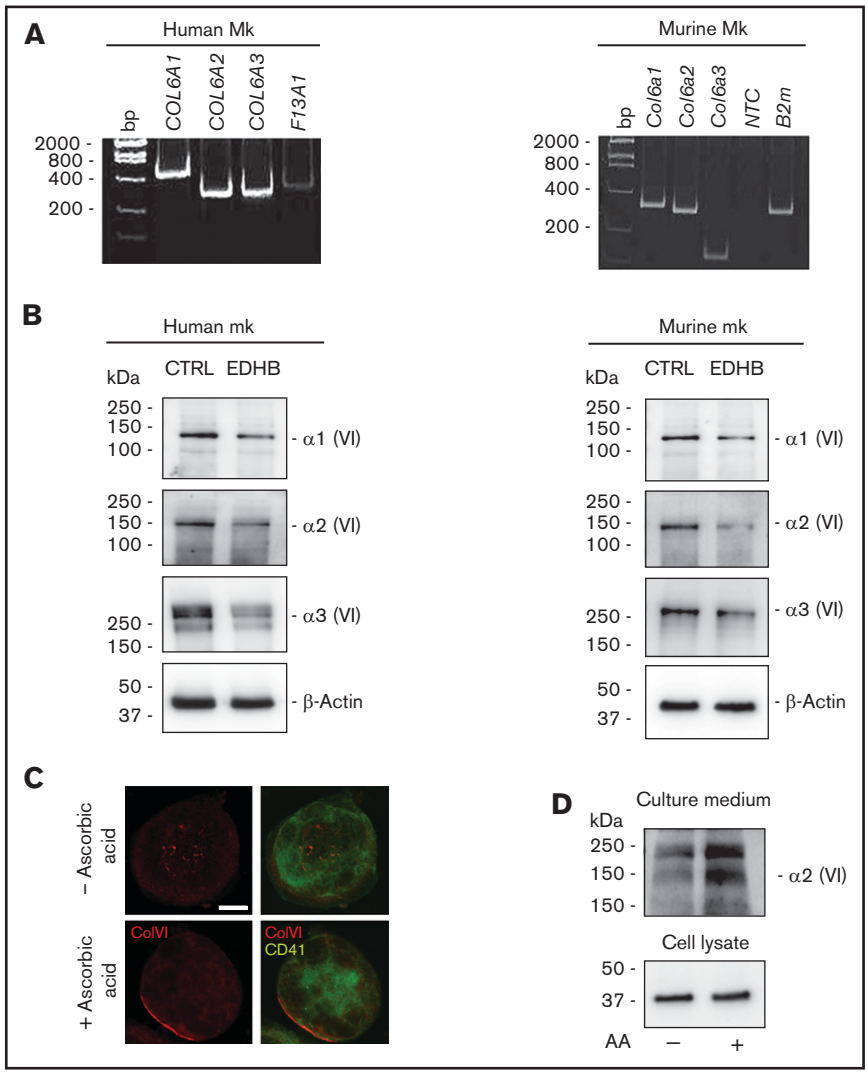

Figure 1. Human and murine Mks express collagen VI. (A) RT-PCR of *COL6A1*, *COL6A2*, and *COL6A3* messenger RNAs in human (left panel) and murine (right panel) Mks. Factor XIII (*F13A1*) and β2-microglobulin (*B2m*) were used as positive controls. The migration of the DNA size marker (bp) is shown. (B) Western blot for α1, α2, and α3 chains of collagen VI in human (left panel) and murine (right panel) Mks. Membranes were probed with monoclonal antibodies raised against each single chain. β-Actin was used as a loading control. Where indicated, Mks were treated with 100 μM the prolyl-4-hydroxylase inhibitor EDHB. In parallel, Mks were treated with vehicle alone (0.1% ethanol) as control. (C) Confocal microscopy immunofluorescence of WT mouse Mks stained with a polyclonal antibody against collagen VI (red) and a monoclonal antibody against CD41 (green). Where indicated, Mks were cultured in the presence of 50 μg/mL ascorbic acid for 48 hours. Scale bar, 10 μm. (D) Western blot analysis of collagen VI secretion in the culture medium by Mks. Differentiated WT Mks were cultured for 48 hours in the absence or presence of 50 μg/mL ascorbic acid (AA). Then, the culture medium was collected, centrifuged, and resolved using sodium dodecyl sulfate polyacrylamide gel electrophoresis under reducing and denaturing conditions. Membranes were probed with a monoclonal antibody recognizing collagen VI α2 chain. CTRL, control; NTC, no template control; VI, collagen VI.

and analyzed. *Col6a1*$^{-/-}$ Mks maintained increased expression of STIM1 and ORAI1, as demonstrated by quantitative RT-PCR (qRT-PCR) and flow cytometry (Figure 5A). These alterations were transferred to platelets, as indicated by western blot for STIM1 and ORAI1 (Figure 5B). Also, platelets isolated from WT mice that were transplanted with *Col6a1*$^{-/-}$ Lin^{-} BM cells showed increased levels of phosphorylated (p)S6 and p4E-BP1 (supplemental Figure 5). Platelets produced by *Col6a1*$^{-/-}$ Mks in a WT BM environment maintained the increased susceptibility to activation, relative to WT platelets, as demonstrated by αIIbβ3 activation and CD62P (P-selectin) exposure on the cell membrane after stimulation with major agonists (thrombin, ADP, and CVX) (Figure 5C).

Rapamycin treatment normalizes STIM1 and ORAI1 expression and SOCE

To test whether the increased expression of SOCE effectors was directly dependent on mTORC1 signaling, we cultured flushed BM cells from WT and *Col6a1*$^{-/-}$ mice in the presence of thrombopoietin to induce Mk differentiation and treated them

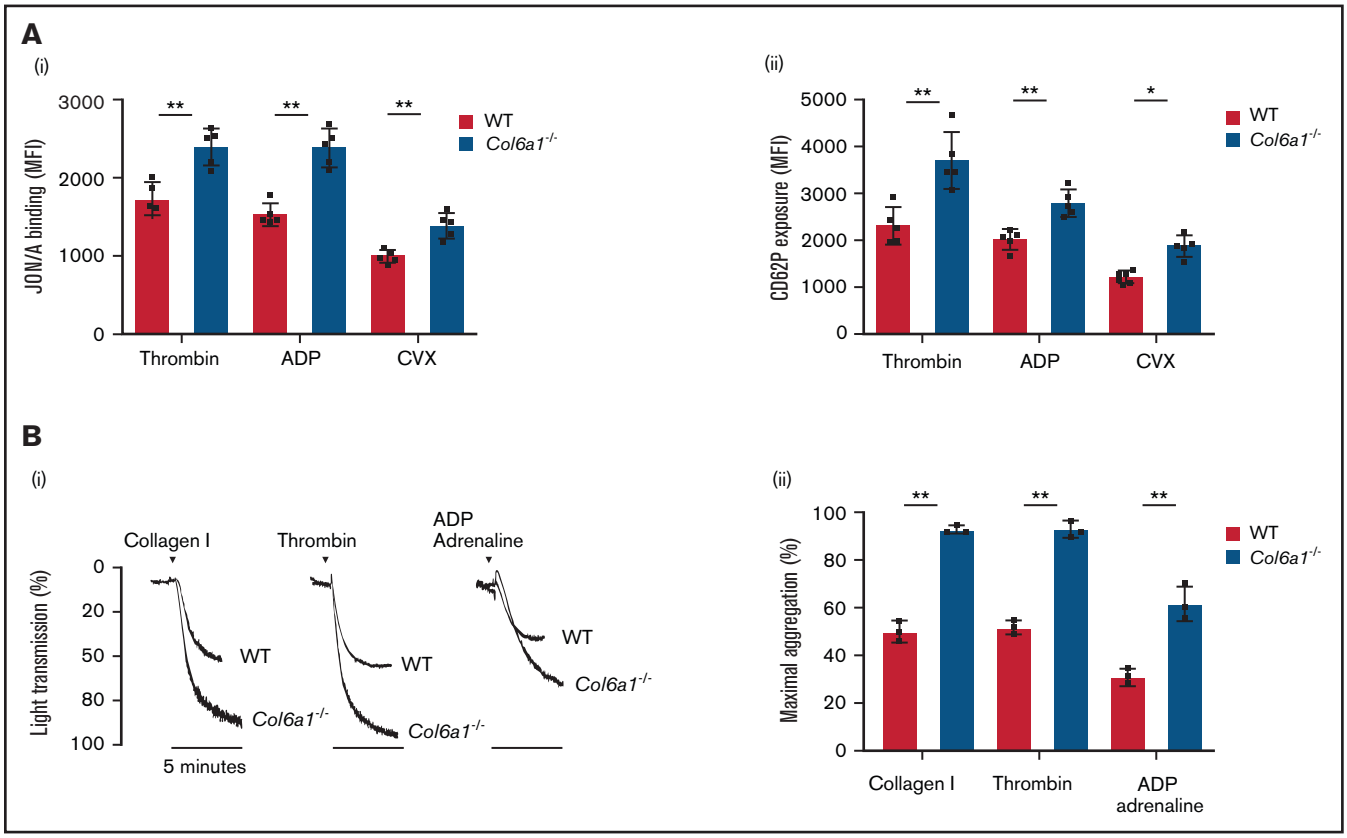

Figure 2. *Col6a1*$^{-/-}$ platelets display an increased tendency toward activation and aggregation. (A) Platelet activation response in platelets from WT and *Col6a1*$^{-/-}$ mice, measured 10 minutes after stimulation with 0.1 U/mL thrombin, 25 μM ADP, or 20 ng/mL CVX. Platelet activation was detected by the binding of the JON/A antibody against activated integrin αIIbβ3 (Ai) and the binding of the anti-CD62P antibody (Aii). Data are mean ± SD (n = 5). Student *t* test. (Bi) Representative aggregation response of washed platelets (1.7×10^5/μL) prepared from WT and *Col6a1*$^{-/-}$ mice. Platelets were stimulated with different agonists (collagen I 5 μg/mL, thrombin 0.5 U/mL, and ADP plus adrenaline 20 μM each, in the presence of 1 mM $CaCl_2$. Platelet aggregation was measured as a change in light transmission using a lumi-aggregometer. (Bii) Quantification of the percentage of maximal platelet aggregation. Data are mean ± SD (n = 3). Student *t* test. *$P < .05$, **$P < .01$. MFI, mean fluorescence intensity.

with the mTOR inhibitor rapamycin or with vehicle alone. Mks were purified by gradient sedimentation and lysed. Western blot analysis confirmed higher protein levels of STIM1 and ORAI1 in *Col6a1*$^{-/-}$ Mks (Figure 6A). Rapamycin treatment induced a significant reduction in STIM1 and ORAI1 levels (Figure 6A), with a consequent reduction in CPA-induced SOCE activation (Figure 6B) that was similar in WT and *Col6a1*$^{-/-}$ Mks following rapamycin treatment. mTOR signaling was assessed in vivo by injecting mice with rapamycin or vehicle. In vivo, rapamycin treatment resulted in a significant reduction in pS6 and p4E-BP1 in *Col6a1*$^{-/-}$ platelets to a level comparable to WT platelets under resting conditions and after stimulation with thrombin (supplemental Figure 6). In vivo, rapamycin administration also resulted in a normalization of STIM1 and ORAI1 protein expression in *Col6a1*$^{-/-}$ BM Mks (Figure 6C; supplemental Figure 7) and platelets (Figure 6D). The reduction in the expression of SOCE effectors resulted in a significant decrease in platelet activation upon thrombin stimulation, detected by active integrin αIIbβ3, to a level comparable to WT platelets (Figure 6E). Rapamycin treatment also normalized the peripheral blood platelet count of *Col6a1*$^{-/-}$ mice, which showed a mild thrombocytopenia (Figure 6F).

Platelets derived from patients harboring collagen VI mutations show increased levels of SOCE effectors

We analyzed peripheral blood platelets derived from healthy subjects and patients affected by Bethlem myopathy and UCMD of intermediate severity (Table 1). The phosphorylation of S6 ribosomal protein and of 4E-BP1 appeared significantly increased in platelets isolated from patients, relative to those isolated from healthy subjects (Figure 7A). Further, the amounts of STIM1 and ORAI1 proteins were increased in patient platelets compared with healthy subjects (Figure 7B). Additionally, when we tested platelet activation in response to thrombin stimulation, we observed increased activation of integrin αIIbβ3 in patients compared with healthy subjects (Figure 7C).

Discussion

The release of functional platelets from Mks is regulated by environmental and autocrine factors.[17,20,48-50] In previous studies, we demonstrated that Mks express different extracellular matrix components that regulate platelet production.[37,51] Here, we demonstrated that

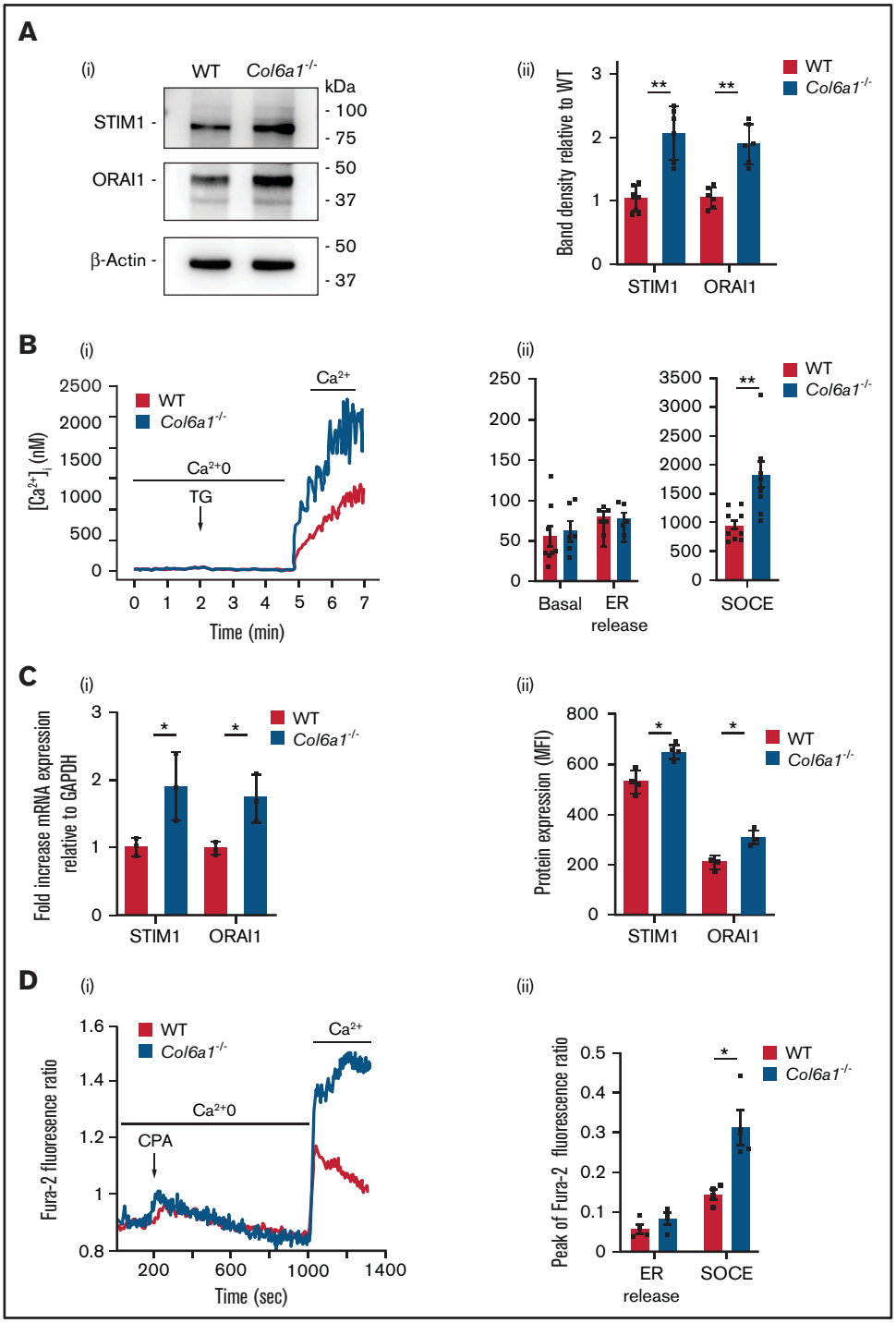

Figure 3. *Col6a1*$^{-/-}$ platelets and Mks have increased STIM1 and ORAI1 expression and increased SOCE. (Ai) Western blot for STIM1 and ORAI1 in WT and *Col6a1*$^{-/-}$ platelets. β-Actin was used as a loading control. (Aii) Band densities were quantified and expressed relative to WT. Data are mean ± SD ($n = 6$). Student *t* test. (Bi) Representative FLUO3 fluorescence–based $[Ca^{2+}]_i$ traces of WT (red line) and *Col6a1*$^{-/-}$ (blue line) platelets incubated in $Ca^{2+}0$ conditions. Where indicated, successive additions of 5 μM thapsigargin (TG) and 1 mM Ca^{2+} were carried out. (Bii) Quantification of basal and peak $[Ca^{2+}]_i$ following the addition of thapsigargin (ER release) and Ca^{2+} (SOCE) in WT and *Col6a1*$^{-/-}$ platelets. Data are mean ± SEM ($n = 5$). Student *t* test. (Ci) Quantitative RT-PCR analysis of STIM1 and ORAI1 mRNA expression in sorted BM Mks from WT and *Col6a1*$^{-/-}$ mice. Data are mean ± SD ($n = 3$). Student *t* test. (Cii) Flow cytometry analysis of STIM1 and ORAI1 protein levels in BM Mks from WT and *Col6a1*$^{-/-}$ mice. Data are mean ± SD ($n = 4$). Student *t* test. (Di) Representative Fura-2 fluorescence ratios reflecting $[Ca^{2+}]_i$ in WT and *Col6a1*$^{-/-}$ differentiated Mks. $[Ca^{2+}]_i$ variations were monitored in the presence of 10 μM CPA in $Ca^{2+}0$ and after addition of 1.5 mM extracellular Ca^{2+}. (Dii) Analysis of Ca^{2+} flows (ER release and SOCE) in WT and *Col6a1*$^{-/-}$ Mks. Data are mean ± SEM ($n = 4$). Student *t* test. *$P < .05$, **$P < .01$.

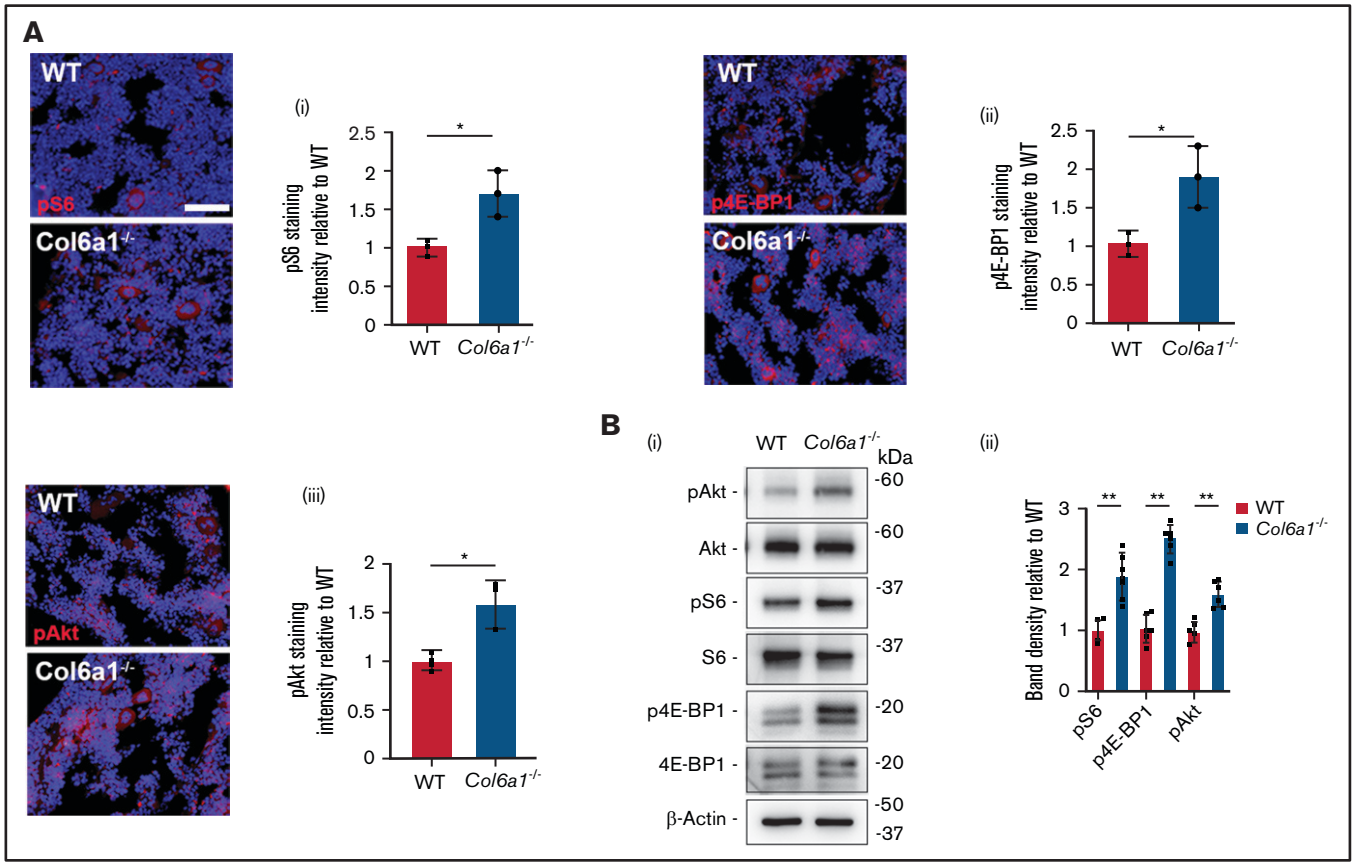

Figure 4. *Col6a1*$^{-/-}$ Mks and platelets display increased mTORC1 signaling. (A) In situ staining of phosphorylated (p)S6 protein (i), p4E-BP1 protein (ii), and pAkt (iii) in WT and *Col6a1*$^{-/-}$ CD41^{+} BM Mks. Staining intensities were quantified and expressed relative to WT. A minimum of 40 Mks were analyzed per section. Data are mean ± SD (n = 3). Student *t* test. (Bi) Western blot of pAkt, pS6, and p4E-BP1 in WT and *Col6a1*$^{-/-}$ platelets. Total Akt, total S6, total 4E-BP1, and β-actin were used as loading controls. (Bii) Band densities were quantified and expressed relative to WT. Data are mean ± SD (n = 6). Student *t* test. *$P < .05$; ** $P < .01$.

human and mouse Mks express collagen VI, as confirmed by 3 recent studies.[52-54] In this study, we took advantage of a collagen VI–null mouse model and found that *Col6a1*$^{-/-}$ platelets display a hyperactivation tendency, as revealed by different in vitro tests that we conducted. Based on our results, this phenotype is due to an intrinsic platelet defect because the platelet function tests were performed on washed platelets that were devoid of extrinsic factors involved in platelet activation and aggregation (eg, plasma, interaction with other cells, blood flow rate). Platelet activation and aggregation are directly dependent on an increase in $[Ca^{2+}]_i$. The SOCE mechanism has a major role in regulating intracellular Ca^{2+} content in platelets through the coordinated action of its main effectors STIM1 and ORAI1.[20,21] Contrary to platelets derived from mice with a constitutive activation of Stim1,[15] in *Col6a1*$^{-/-}$ platelets we observed a normal basal level of cytosolic calcium. Also, the level of Ca^{2+} released by the ER, upon SERCA inhibition, in *Col6a1*$^{-/-}$ platelets was normal. In collagen VI–null platelets, the increased expression of STIM1 and ORAI1 resulted in a higher level of cytosolic Ca^{2+} influx from the extracellular space upon SOCE activation. The consequent increase in $[Ca^{2+}]_i$ leads to increased platelet reactivity.[15,55,56]

We previously proved that Mks express STIM1 and ORAI1 and that an increase in $[Ca^{2+}]_i$ prompted by SOCE activation is crucial to promote proplatelet extension and platelet release.[16,57] In this study, we found overexpression of STIM1 and ORAI1 and increased SOCE in *Col6a1*$^{-/-}$ Mks, indicating that the defects displayed in collagen VI–null platelets may originate from Mks.

It was demonstrated previously that STIM1 and ORAI1 expression is under the control of the mTOR pathway.[27,28] A distinctive signaling defect found in *Col6a1*$^{-/-}$ tissues is the hyperactivation of the Akt/mTOR pathway, which, in turn, results in autophagy deregulation.[10,58,59] mTOR includes 2 complexes: mTORC1 and mTORC2.[60] mTORC1 activation, through the PI3K/Akt/mTOR-mediated phosphorylation of 4E-BP1 and S6, regulates protein synthesis.[61] The mTOR pathway was proven to positively regulate platelet activation and aggregation, as well as thrombus formation and platelet aggregate stability, by regulating protein synthesis.[32,62,63]

Constitutive mTOR activation stimulates mitochondrial biogenesis and function and, consequently, reactive oxygen species (ROS) production.[64] Higher levels of platelet ROS are associated with increased platelet activation, and ROS scavenger administration reduces platelet activation in aged mice, which are characterized by increased mTOR signaling activity.[65] In addition, a reciprocal interplay between SOCE and mitochondria has been reported because cytosolic calcium oscillations are decoded in the mitochondria.[66] Thus, the increase in cytosolic calcium upon SOCE activation, as

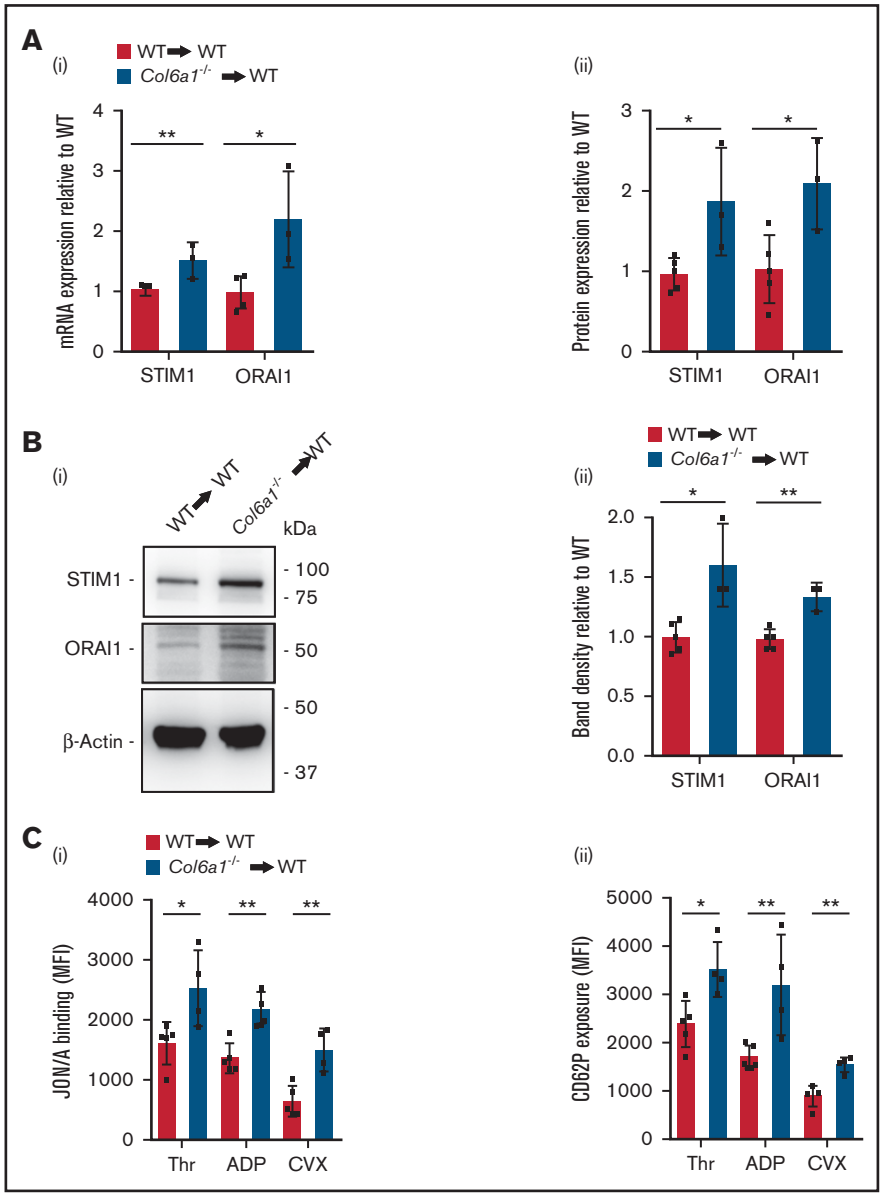

Figure 5. *Col6a1*$^{-/-}$ Mks and platelets maintain SOCE alterations after BM transplantation in a WT background. (Ai) qRT-PCR analysis of STIM1 and ORAI1 mRNA expression in sorted BM Mks from WT recipient mice after BM transplantation with WT (WT→WT) or *Col6a1*$^{-/-}$ (*Col6a1*$^{-/-}$→WT) Lin^{-} BM cells. Data are mean ± SD (WT→WT, n = 5; *Col6a1*$^{-/-}$→WT, n = 3). Student *t* test. (Aii) Flow cytometry analysis of STIM1 and ORAI1 protein levels in BM Mks from WT recipient mice after BM transplantation, as in (i). Data are mean ± SD (WT→WT, n = 5; *Col6a1*$^{-/-}$→WT, n = 3). Student *t* test. (Bi) Western blot for STIM1 and ORAI1 in platelets isolated from WT recipient mice after BM transplantation with WT or *Col6a1*$^{-/-}$ Lin^{-} BM cells, as in (A). β-Actin was used as a loading control. (Bii) Band densities were quantified and expressed relative to WT→WT. Data are mean ± SD (WT→WT, n = 5; *Col6a1*$^{-/-}$→WT, n = 3). Student *t* test. (C) Platelet activation measured as integrin αIIbβ3 activation (i) and CD62P cell surface exposure (ii) after stimulation with 0.1 U/mL thrombin (Thr), 25 μM ADP, or 20 ng/mL CVX in platelets isolated from WT recipient mice after transplantation with WT or *Col6a1*$^{-/-}$ Lin^{-} BM cells. Data are mean ± SD (WT→WT, n = 5; *Col6a1*$^{-/-}$→WT, n = 4). Student *t* test. *$P < .05$, **$P < .01$. MFI, mean fluorescence intensity.

observed in *Col6a1*$^{-/-}$ Mks and platelets, might result in an imbalance in intracellular Ca^{2+} dynamics between organelles deputed to Ca^{2+} handling. Future studies will unravel whether STIM1 and ORAI1 overexpression may interfere with the mitochondrial function in *Col6a1*$^{-/-}$ Mks.

To understand whether the endogenous Mk self-produced collagen VI was the principal regulator of functional platelet production, we produced radiation chimeras by transplanting BM Lin^{-} cells from *Col6a1*$^{-/-}$ mice into WT recipients. At 7 to 8 weeks posttransplant, when peripheral blood count was recovered, BM sorted *Col6a1*$^{-/-}$ Mks showed increased expression of STIM1 and ORAI1, despite having undergone differentiation in the presence of collagen VI in the BM environment. As in *Col6a1*$^{-/-}$ mice, STIM1 and ORAI1 overexpression in Mks resulted in the production of platelets with increased susceptibility to activation and overexpressing pS6 and

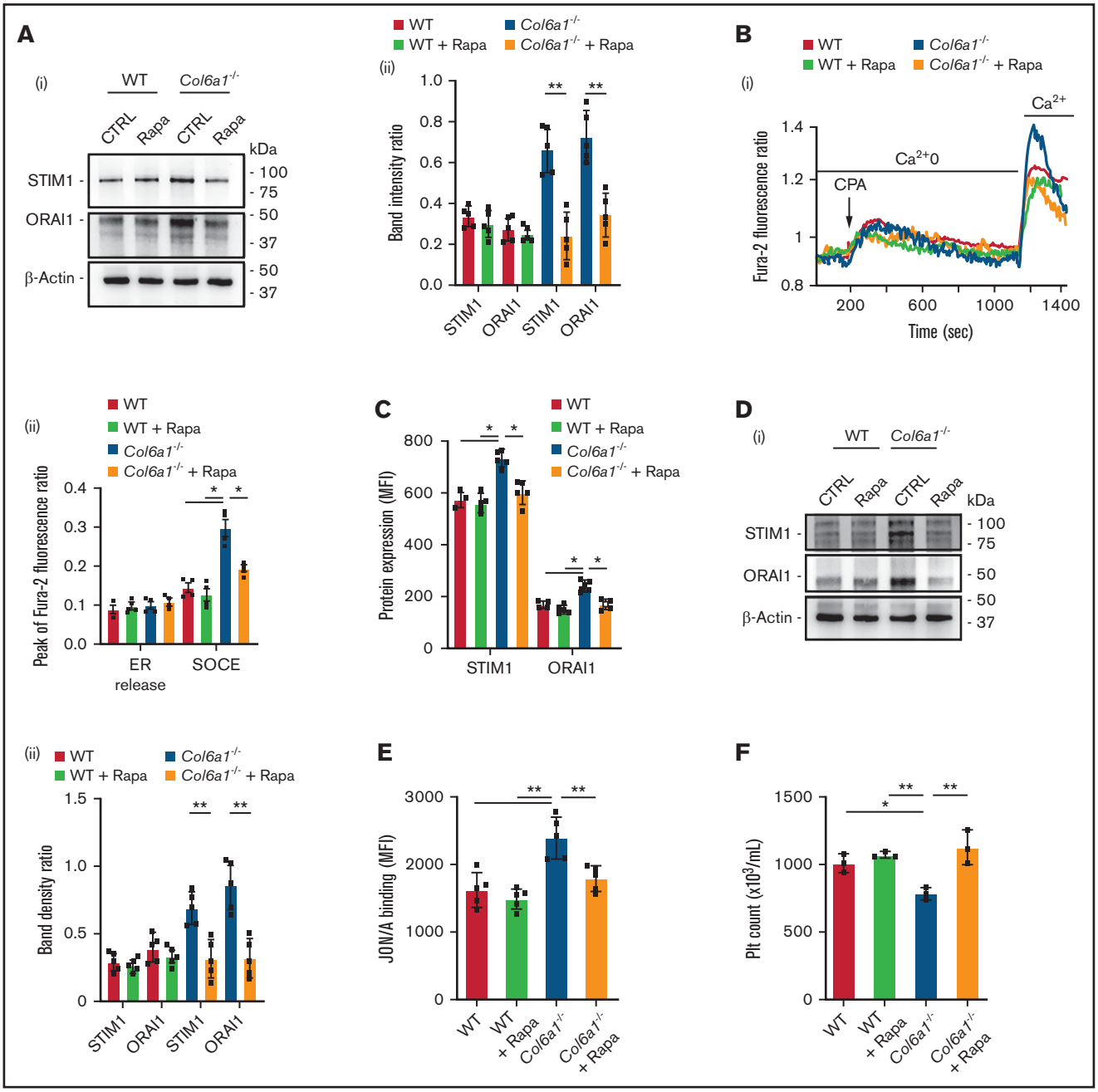

Figure 6. In vitro and in vivo rapamycin treatment normalizes STIM1 and ORAI1 expression and SOCE in *Col6a1*$^{-/-}$ Mks. (Ai) Western blot for STIM1 and ORAI1 in WT and *Col6a1*$^{-/-}$ differentiated Mks, in the presence of 100 nM rapamycin (Rapa) or vehicle alone as control (0.1% DMSO). β-Actin was used as a loading control. (Aii) Band densities were quantified and expressed relative to control. Data are mean ± SD (n = 5). 1-way ANOVA. (Bi) Representative Fura-2 fluorescence ratios reflecting $[Ca^{2+}]_i$ variations in WT and *Col6a1*$^{-/-}$ differentiated Mks, in the presence of 100 nM Rapa or vehicle alone. Ca^{2+} flows were monitored in the presence of 10 μM CPA in $Ca^{2+}0$ conditions and after the addition of 1.5 mM extracellular Ca^{2+}. (Bii) Analysis of Ca^{2+} flows (ER release and SOCE) in WT and *Col6a1*$^{-/-}$ Mks. A minimum of 40 Mks were analyzed per experiment. Data are mean ± SEM (n = 4). 1-way ANOVA. (C) Flow cytometry analysis of STIM1 and ORAI1 protein expression in BM Mks from WT and *Col6a1*$^{-/-}$ mice treated with Rapa (2 mg/kg body weight) or vehicle as control (5% PEG-400/5% Tween-80 in saline). Data are mean ± SD (n = 5). 1-way ANOVA. (Di) Western blot for STIM1 and ORAI1 in platelets from WT and *Col6a1*$^{-/-}$ mice treated with Rapa or vehicle as control. (Dii) Band densities were quantified and expressed relative to control. Data are mean ± SD (n = 5). 1-way ANOVA. (E) Flow cytometry analysis of integrin αIIbβ3 activation (JON/A antibody binding) in WT and *Col6a1*$^{-/-}$ platelets, after stimulation with thrombin (0.1 U/mL), from mice treated with Rapa or vehicle as control. Data are mean ± SD (n = 5). 1-way ANOVA. (F) Peripheral blood platelet (Plt) count in WT and *Col6a1*$^{-/-}$ mice following administration of Rapa or vehicle as control (n = 3). Data are mean ± SD (n = 3). 1-way ANOVA. *P < .05, **P < .01. CTRL, control; MFI, mean fluorescence intensity.

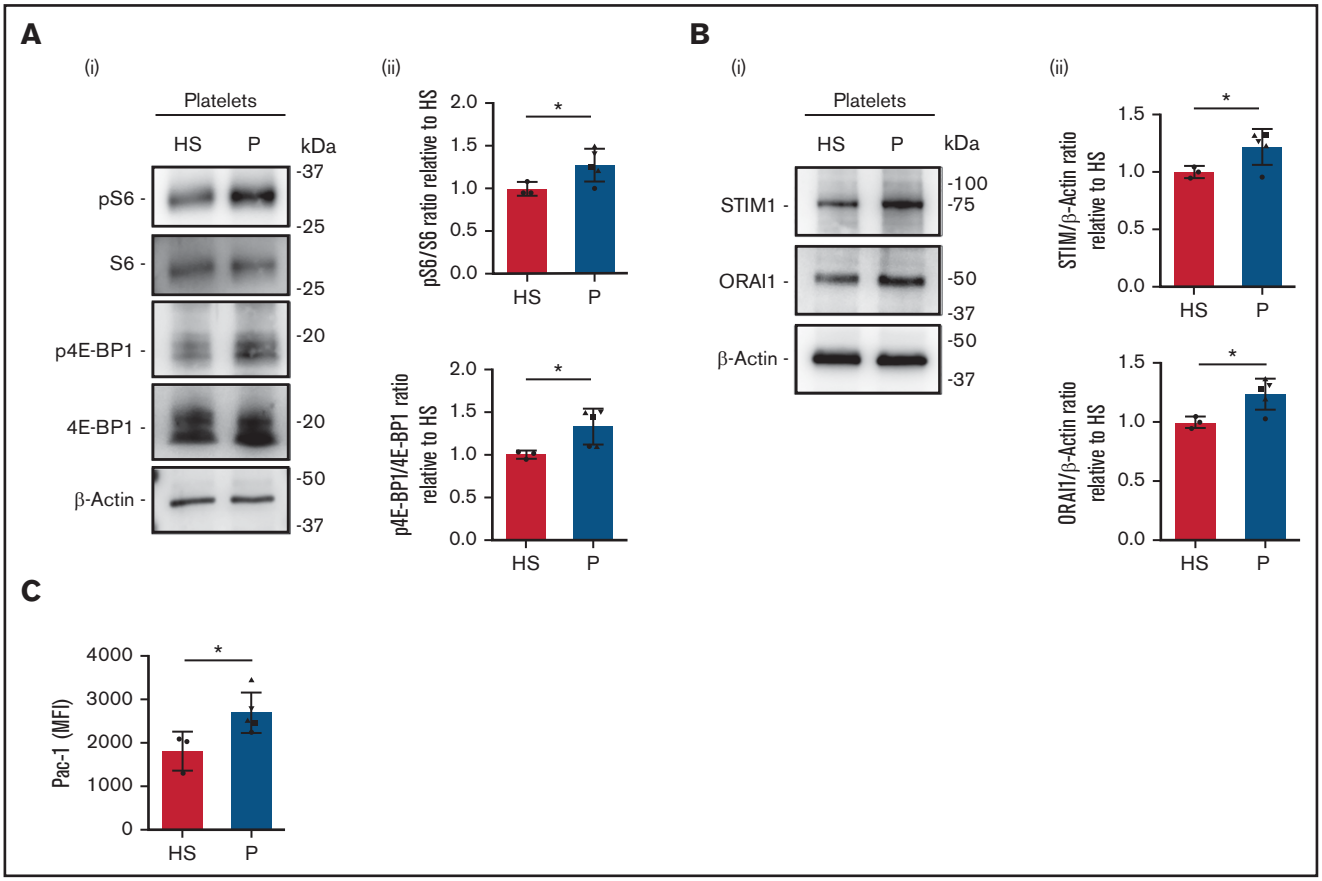

Figure 7. Increased STIM1 and ORAI1 expression in platelets derived from patients affected by collagen VI–related disorders. (Ai) Representative western blot of phosphorylated (p) S6 protein and 4E-BP1 protein in peripheral blood platelets of healthy subjects (HS; n = 3) and patients (P) with Bethlem myopathy/UCMD (n = 5). (Aii) Band densities were quantified and expressed relative to HS. Data are mean ± SD. Student *t* test. (Bi) Representative western blot of STIM1 and ORAI1 protein expression in peripheral blood platelets from HS (n = 3) and P with Bethlem myopathy/UCMD (n = 5). (Bii) Band densities were quantified and expressed relative to HS. Data are mean ± SD. Student *t* test. (C) Flow cytometry analysis of integrin αIIbβ3 activation (PAC-1 antibody binding) in peripheral blood platelets from HS (n = 3) and P with Bethlem myopathy/UCMD (n = 5) after stimulation with thrombin (0.5 U/mL). Data are mean ± SD. Student *t* test. △, patient 1/F; ■, patient 2/M; ●, patient 3/M; ▼, patient 4/F; ▲, patient 5/F. Student *t* test. *$P < .05$. MFI, mean fluorescence intensity.

p4E-BP1. These results proved that the Mk self-produced collagen VI plays a significant role in the production of functional platelets, despite the composition of the BM extracellular matrix environment.

mTOR may have an immediate effect on thrombus formation and stability through a mechanism independent from mRNA translation.[31] Our data show that in vitro and in vivo inhibition of the mTOR signaling by rapamycin treatment restores STIM1 and ORAI1 expression and SOCE in *Col6a1*$^{-/-}$ Mks, leading to a normalization of the platelet activation response. Platelet function abnormalities have been described in patients affected by connective tissue disorders, such as collagenopathies; however, the mechanisms underlying these defects remain unknown.[11,12,67,68] We revealed that peripheral blood platelets of patients affected by collagen VI–related diseases express higher levels of STIM1 and ORAI1, resulting in a hyperactivation state. Interestingly, platelet count was normal in all of the analyzed patients.

No platelet alterations were previously reported for Bethlem myopathy or UCMD. On the other hand, platelet abnormalities are well known in patients harboring gain-of-function mutations in ORAI1 or STIM1 and displaying a multisystemic clinical phenotype that is characterized by muscle weakness, with a clinical spectrum ranging from isolated tubular aggregate myopathy to the more complex Stormorken syndrome (STRMK) or York syndrome.[69] A characteristic feature of STRMK is a mild to pronounced thrombocytopenia and thrombocytopathy. Platelets from patients with STRMK were found to be in an activated state, with increased levels of CD63 and CD62P, whereas other aspects of platelet function are impaired.[69,70] Despite platelet activation and increased SOCE, no thrombotic episodes were observed in patients with STRMK, with only 1 patient presenting with pulmonary embolism and thrombosis.[71] While, it has been observed a rather common bleeding tendency, possibly related to thrombocytopenia and abnormal platelet function. Patients with STRMK or with collagen VI–related diseases showed increased platelet activation, which may suggest an increased thrombotic predisposition. A mild bleeding tendency, which is well established in STRMK, may also be present in patients affected by collagen VI–related myopathies (Table 1). Consistent with this hypothesis, we observed a significantly prolonged

bleeding time in *Col6a1*$^{-/-}$ mice with respect to WT mice in a tail bleeding assay (supplemental Figure 8). This apparent paradox could be explained, in part, by considering the documented key role of collagen VI on platelet adhesion and aggregation under low and high shear conditions. By linking the subendothelial basement membrane to the interstitial collagen network, collagen VI microfilaments play a pivotal role in the hemostatic process that is triggered upon the damage of blood vessels.[72,73] Additional and further studies in larger patient populations are needed to establish whether and to what extent patients affected by collagen VI–related disorders have a risk for bleeding.[15,74] Nevertheless, these data suggest that mutations in different genes resulting in deregulation of Ca^{2+} entry may underlie a shared pathophysiological mechanism involving muscle and platelets.

In conclusion, our data provide a fundamental step toward understanding the interaction between self-produced collagen VI and Ca^{2+} signaling in the regulation of Mk function and production of functional platelets. These data represent clinically relevant evidence to be taken into account for the long-term management of patients affected by collagen VI–related diseases, including Bethlem myopathy and UCMD.

Acknowledgments

The authors thank Cesare Perotti for supplying human cord blood.

This work was supported by the Cariplo Foundation (2013-0717), ERA-Net for Research Programmes on Rare Diseases (EUPLANE), 'Progetti Di Ricerca Di Rilevante Interesse Nazionale' (PRIN 2017Z5LR5Z), the Italian Ministry of Health (Ricerca Finalizzata Giovani Ricercatori GR-2016-02363136). Fellowships awarded to V.A. and C.A.D.B. were funded by Collegio Ghislieri, Pavia, progetto "Progressi in Biologia e Medicina." The authors acknowledge support from the Telethon BioBank (GTB12001D) and the EuroBioBank network.

The funders had no role in the study design, data collection and analysis, decision to publish, or preparation of the manuscript.

Authorship

Contribution: V.A. conceived the study, designed and performed experiments, analyzed data and wrote the manuscript; C.G. designed and performed the experiments, analyzed data, and edited the manuscript; M.B., A.Z., C.A.D.B., M.C., P.-A.L., and E.L. performed experiments, analyzed data, and edited the manuscript; M.M., F.M., V.P., P. Braghetta, and P. Bernardi analyzed data and edited the manuscript; C.S., L.B., and E.P. provided patient samples and analyzed data; L.S. and A.V. assisted with radiation chimeras, analyzed data, and edited the manuscript; L.D.M. and P. Bonaldo designed experiments, analyzed data, and edited the manuscript; and A.B. conceived the study, designed experiments, analyzed data, supervised the project, and wrote the manuscript.

Conflict-of-interest disclosure: The authors declare no competing financial interests.

ORCID profiles: V.A., 0000-0001-8066-9895; C.A.D.B., 0000-0002-6472-2008; P.-A.L., 0000-0002-1435-9298; C.S., 0000-0003-0870-1349; E.L., 0000-0002-3688-9281; V.P., 0000-0003-4026-6404; A.V., 0000-0003-4428-9013; L.B., 0000-0002-3075-6525; P. Bernardi, 0000-0001-9187-3736; P. Braghetta, 0000-0003-2547-8679; P. Bonaldo, 0000-0002-9571-8140; A.B., 0000-0003-3145-1245.

Correspondence: Alessandra Balduini, University of Pavia, via Forlanini 6, 27100 Pavia, Italy; e-mail: alebal04@unipv.it.

References

1. Cescon M, Gattazzo F, Chen P, Bonaldo P. Collagen VI at a glance. *J Cell Sci.* 2015;128(19):3525-3531.
2. Fitzgerald J, Rich C, Zhou FH, Hansen U. Three novel collagen VI chains, alpha4(VI), alpha5(VI), and alpha6(VI). *J Biol Chem.* 2008;283(29):20170-20180.
3. Gara SK, Grumati P, Urciuolo A, et al. Three novel collagen VI chains with high homology to the alpha3 chain. *J Biol Chem.* 2008;283(16):10658-10670.
4. Bönnemann CG. The collagen VI-related myopathies: muscle meets its matrix. *Nat Rev Neurol.* 2011;7(7):379-390.
5. Bonaldo P, Braghetta P, Zanetti M, Piccolo S, Volpin D, Bressan GM. Collagen VI deficiency induces early onset myopathy in the mouse: an animal model for Bethlem myopathy. *Hum Mol Genet.* 1998;7(13):2135-2140.
6. Bernardi P, Bonaldo P. Dysfunction of mitochondria and sarcoplasmic reticulum in the pathogenesis of collagen VI muscular dystrophies. *Ann N Y Acad Sci.* 2008;1147(1):303-311.
7. Irwin WA, Bergamin N, Sabatelli P, et al. Mitochondrial dysfunction and apoptosis in myopathic mice with collagen VI deficiency. *Nat Genet.* 2003;35(4):367-371.
8. Cescon M, Chen P, Castagnaro S, Gregorio I, Bonaldo P. Lack of collagen VI promotes neurodegeneration by impairing autophagy and inducing apoptosis during aging. *Aging (Albany NY).* 2016;8(5):1083-1101.
9. Chen P, Cescon M, Zuccolotto G, et al. Collagen VI regulates peripheral nerve regeneration by modulating macrophage recruitment and polarization. *Acta Neuropathol.* 2015;129(1):97-113.
10. Castagnaro S, Chrisam M, Cescon M, Braghetta P, Grumati P, Bonaldo P. Extracellular collagen VI has prosurvival and autophagy instructive properties in mouse fibroblasts. *Front Physiol.* 2018;9:1129.
11. Artoni A, Bassotti A, Abbattista M, et al. Hemostatic abnormalities in patients with Ehlers-Danlos syndrome. *J Thromb Haemost.* 2018;16(12):2425-2431.

12. Estes JW. Platelet abnormalities in heritable disorders of connective tissue. *Ann N Y Acad Sci.* 1972;201(1):445-450.
13. Malfait F, De Paepe A. Bleeding in the heritable connective tissue disorders: mechanisms, diagnosis and treatment. *Blood Rev.* 2009;23(5):191-197.
14. Münzer P, Walker-Allgaier B, Geue S, et al. CK2β regulates thrombopoiesis and Ca^{2+}-triggered platelet activation in arterial thrombosis. *Blood.* 2017;130(25):2774-2785.
15. Grosse J, Braun A, Varga-Szabo D, et al. An EF hand mutation in Stim1 causes premature platelet activation and bleeding in mice. *J Clin Invest.* 2007;117(11):3540-3550.
16. Di Buduo CA, Moccia F, Battiston M, et al. The importance of calcium in the regulation of megakaryocyte function. *Haematologica.* 2014;99(4):769-778.
17. Abbonante V, Di Buduo CA, Gruppi C, et al. A new path to platelet production through matrix sensing. *Haematologica.* 2017;102(7):1150-1160.
18. Mahaut-Smith MP. The unique contribution of ion channels to platelet and megakaryocyte function. *J Thromb Haemost.* 2012;10(9):1722-1732.
19. Taylor CW. Store-operated Ca2+ entry: A STIMulating stOrai. *Trends Biochem Sci.* 2006;31(11):597-601.
20. Di Buduo CA, Balduini A, Moccia F. Pathophysiological significance of store-operated calcium entry in megakaryocyte function: opening new paths for understanding the role of calcium in thrombopoiesis. *Int J Mol Sci.* 2016;17(12):2055.
21. Varga-Szabo D, Braun A, Nieswandt B. Calcium signaling in platelets. *J Thromb Haemost.* 2009;7(7):1057-1066.
22. Borst O, Schmidt EM, Münzer P, et al. The serum- and glucocorticoid-inducible kinase 1 (SGK1) influences platelet calcium signaling and function by regulation of Orai1 expression in megakaryocytes. *Blood.* 2012;119(1):251-261.
23. Berna-Erro A, Jardín I, Smani T, Rosado JA. Regulation of platelet function by Orai, STIM and TRP. *Adv Exp Med Biol.* 2016;898:157-181.
24. Braun A, Varga-Szabo D, Kleinschnitz C, et al. Orai1 (CRACM1) is the platelet SOC channel and essential for pathological thrombus formation. *Blood.* 2009;113(9):2056-2063.
25. Gilio K, van Kruchten R, Braun A, et al. Roles of platelet STIM1 and Orai1 in glycoprotein VI- and thrombin-dependent procoagulant activity and thrombus formation. *J Biol Chem.* 2010;285(31):23629-23638.
26. Vaeth M, Maus M, Klein-Hessling S, et al. Store-Operated Ca^{2+} entry controls clonal expansion of T cells through metabolic reprogramming. *Immunity.* 2017;47(4):664-679.e6.
27. Ogawa A, Firth AL, Smith KA, Maliakal MV, Yuan JX. PDGF enhances store-operated Ca2+ entry by upregulating STIM1/Orai1 via activation of Akt/mTOR in human pulmonary arterial smooth muscle cells. *Am J Physiol Cell Physiol.* 2012;302(2):C405-C411.
28. Peng H, Liu J, Sun Q, et al. mTORC1 enhancement of STIM1-mediated store-operated Ca2+ entry constrains tuberous sclerosis complex-related tumor development. *Oncogene.* 2013;32(39):4702-4711.
29. Drayer AL, Olthof SG, Vellenga E. Mammalian target of rapamycin is required for thrombopoietin-induced proliferation of megakaryocyte progenitors. *Stem Cells.* 2006;24(1):105-114.
30. Raslova H, Baccini V, Loussaief L, et al. Mammalian target of rapamycin (mTOR) regulates both proliferation of megakaryocyte progenitors and late stages of megakaryocyte differentiation. *Blood.* 2006;107(6):2303-2310.
31. Aslan JE, Tormoen GW, Loren CP, Pang J, McCarty OJ. S6K1 and mTOR regulate Rac1-driven platelet activation and aggregation. *Blood.* 2011;118(11):3129-3136.
32. Weyrich AS, Denis MM, Schwertz H, et al. mTOR-dependent synthesis of Bcl-3 controls the retraction of fibrin clots by activated human platelets. *Blood.* 2007;109(5):1975-1983.
33. Shegogue D, Trojanowska M. Mammalian target of rapamycin positively regulates collagen type I production via a phosphatidylinositol 3-kinase-independent pathway. *J Biol Chem.* 2004;279(22):23166-23175.
34. Zhang Y, Stefanovic B. mTORC1 phosphorylates LARP6 to stimulate type I collagen expression. *Sci Rep.* 2017;7(1):41173.
35. Di Buduo CA, Abbonante V, Tozzi L, Kaplan DL, Balduini A. Three-dimensional tissue models for studying ex vivo megakaryocytopoiesis and platelet production. *Methods Mol Biol.* 2018;1812:177-193.
36. An B, Abbonante V, Xu H, et al. Recombinant collagen engineered to bind to discoidin domain receptor functions as a receptor inhibitor. *J Biol Chem.* 2016;291(9):4343-4355.
37. Abbonante V, Di Buduo CA, Gruppi C, et al. Thrombopoietin/TGF-β1 loop regulates megakaryocyte extracellular matrix component synthesis. *Stem Cells.* 2016;34(4):1123-1133.
38. Bergmeier W, Schulte V, Brockhoff G, Bier U, Zirngibl H, Nieswandt B. Flow cytometric detection of activated mouse integrin alphaIIbbeta3 with a novel monoclonal antibody. *Cytometry.* 2002;48(2):80-86.
39. Marconi C, Di Buduo CA, LeVine K, et al. Loss-of-function mutations in *PTPRJ* cause a new form of inherited thrombocytopenia. *Blood.* 2019;133(12):1346-1357.
40. Di Buduo CA, Abbonante V, Marty C, et al. Defective interaction of mutant calreticulin and SOCE in megakaryocytes from patients with myeloproliferative neoplasms. *Blood.* 2020;135(2):133-144.
41. Urciuolo A, Quarta M, Morbidoni V, et al. Collagen VI regulates satellite cell self-renewal and muscle regeneration. *Nat Commun.* 2013;4(1):1964.
42. Foley AR, Quijano-Roy S, Collins J, et al. Natural history of pulmonary function in collagen VI-related myopathies. *Brain.* 2013;136(Pt 12):3625-3633.
43. Rodeghiero F, Tosetto A, Abshire T, et al. ISTH/SSC bleeding assessment tool: a standardized questionnaire and a proposal for a new bleeding score for inherited bleeding disorders. *J Thromb Haemost.* 2010;8(9):2063–2065.

44. Elbatarny M, Mollah S, Grabell J, et al; Zimmerman Program Investigators. Normal range of bleeding scores for the ISTH-BAT: adult and pediatric data from the merging project. *Haemophilia.* 2014;20(6):831-835.
45. Rocnik EF, Chan BM, Pickering JG. Evidence for a role of collagen synthesis in arterial smooth muscle cell migration. *J Clin Invest.* 1998;101(9): 1889-1898.
46. Cahalan MD. STIMulating store-operated Ca(2+) entry. *Nat Cell Biol.* 2009;11(6):669-677.
47. Lytton J, Westlin M, Hanley MR. Thapsigargin inhibits the sarcoplasmic or endoplasmic reticulum Ca-ATPase family of calcium pumps. *J Biol Chem.* 1991;266(26):17067-17071.
48. Balduini A, Pallotta I, Malara A, et al. Adhesive receptors, extracellular proteins and myosin IIA orchestrate proplatelet formation by human megakaryocytes. *J Thromb Haemost.* 2008;6(11):1900-1907.
49. Semeniak D, Kulawig R, Stegner D, et al. Proplatelet formation is selectively inhibited by collagen type I through Syk-independent GPVI signaling. *J Cell Sci.* 2016;129(18):3473-3484.
50. Machlus KR, Johnson KE, Kulenthirarajan R, et al. CCL5 derived from platelets increases megakaryocyte proplatelet formation. *Blood.* 2016; 127(7):921-926.
51. Malara A, Currao M, Gruppi C, et al. Megakaryocytes contribute to the bone marrow-matrix environment by expressing fibronectin, type IV collagen, and laminin. *Stem Cells.* 2014;32(4):926-937.
52. Chiu SK, Orive SL, Moon MJ, et al. Shared roles for *Scl* and *Lyl1* in murine platelet production and function. *Blood.* 2019;134(10):826-835.
53. Middleton EA, Rowley JW, Campbell RA, et al. Sepsis alters the transcriptional and translational landscape of human and murine platelets. *Blood.* 2019;134(12):911-923.
54. Wang H, He J, Xu C, et al. Decoding Human Megakaryocyte Development. *Cell Stem Cell.* 2021;28(3):535-549.e8.
55. Stefanini L, Paul DS, Robledo RF, et al. RASA3 is a critical inhibitor of RAP1-dependent platelet activation. *J Clin Invest.* 2015;125(4):1419-1432.
56. Stritt S, Beck S, Becker IC, et al. Twinfilin 2a regulates platelet reactivity and turnover in mice. *Blood.* 2017;130(15):1746-1756.
57. Pietra D, Rumi E, Ferretti VV, et al. Differential clinical effects of different mutation subtypes in CALR-mutant myeloproliferative neoplasms. *Leukemia.* 2016;30(2):431-438.
58. Chrisam M, Pirozzi M, Castagnaro S, et al. Reactivation of autophagy by spermidine ameliorates the myopathic defects of collagen VI-null mice. *Autophagy.* 2015;11(12):2142-2152.
59. Grumati P, Coletto L, Sabatelli P, et al. Autophagy is defective in collagen VI muscular dystrophies, and its reactivation rescues myofiber degeneration. *Nat Med.* 2010;16(11):1313-1320.
60. Laplante M, Sabatini DM. mTOR signaling in growth control and disease. *Cell.* 2012;149(2):274-293.
61. Saxton RA, Sabatini DM. mTOR signaling in growth, metabolism, and disease [published correction appears in *Cell.* 2017;169(2):361–371]. *Cell.* 2017;168(6):960-976.
62. Pabla R, Weyrich AS, Dixon DA, et al. Integrin-dependent control of translation: engagement of integrin alphaIIbbeta3 regulates synthesis of proteins in activated human platelets. *J Cell Biol.* 1999;144(1):175-184.
63. Weyrich AS, Dixon DA, Pabla R, et al. Signal-dependent translation of a regulatory protein, Bcl-3, in activated human platelets. *Proc Natl Acad Sci USA.* 1998;95(10):5556-5561.
64. Morita M, Gravel SP, Chénard V, et al. mTORC1 controls mitochondrial activity and biogenesis through 4E-BP-dependent translational regulation. *Cell Metab.* 2013;18(5):698-711.
65. Yang J, Zhou X, Fan X, et al. mTORC1 promotes aging-related venous thrombosis in mice via elevation of platelet volume and activation. *Blood.* 2016;128(5):615-624.
66. Hajnóczky G, Robb-Gaspers LD, Seitz MB, Thomas AP. Decoding of cytosolic calcium oscillations in the mitochondria. *Cell.* 1995;82(3):415-424.
67. Jiménez-Encarnación E, Vilá LM. Recurrent venous thrombosis in Ehlers-Danlos syndrome type III: an atypical manifestation. *BMJ Case Rep.* 2013; 2013:bcr2013008922.
68. Malfait F, De Paepe A. Bleeding in the heritable connective tissue disorders: mechanisms, diagnosis and treatment. *Blood Rev.* 2009;23(5):191-197.
69. Lacruz RS, Feske S. Diseases caused by mutations in ORAI1 and STIM1. *Ann N Y Acad Sci.* 2015;1356(1):45-79.
70. Markello T, Chen D, Kwan JY, et al. York platelet syndrome is a CRAC channelopathy due to gain-of-function mutations in STIM1. *Mol Genet Metab.* 2015;114(3):474-482.
71. Misceo D, Holmgren A, Louch WE, et al. A dominant STIM1 mutation causes Stormorken syndrome. *Hum Mutat.* 2014;35(5):556-564.
72. Manon-Jensen T, Kjeld NG, Karsdal MA. Collagen-mediated hemostasis. *J Thromb Haemost.* 2016;14(3):438-448.
73. Mazzucato M, Spessotto P, Masotti A, et al. Identification of domains responsible for von Willebrand factor type VI collagen interaction mediating platelet adhesion under high flow. *J Biol Chem.* 1999;274(5):3033-3041.
74. Jarre A, Gowert NS, Donner L, et al. Pre-activated blood platelets and a pro-thrombotic phenotype in APP23 mice modeling Alzheimer's disease. *Cell Signal.* 2014;26(9):2040-2050.